

Generalized Three-Sphere Microswimmers

Kento Yasuda,¹ Yuto Hosaka,² and Shigeyuki Komura^{3,4,5,*}

¹Research Institute for Mathematical Sciences, Kyoto University, Kyoto 606-8502, Japan

²Max Planck Institute for Dynamics and Self-Organization (MPI DS), Am Fassberg 17, 37077 Göttingen, Germany

³Wenzhou Institute, University of Chinese Academy of Sciences, Wenzhou, Zhejiang 325001, China

⁴Oujiang Laboratory, Wenzhou, Zhejiang 325000, China

⁵Department of Chemistry, Graduate School of Science, Tokyo Metropolitan University, Tokyo 192-0397, Japan

Among several models for microswimmers, the three-sphere microswimmer proposed by Najafi and Golestanian captures the essential mechanism for the locomotion of a microswimmer in a viscous fluid. Owing to its simplicity and flexibility, the original three-sphere model has been extended and generalized in various ways to discuss new swimming mechanisms of microswimmers. We shall provide a systematic and concise review of the various extensions of the three-sphere microswimmers that have been developed by the present authors. In particular, we shall discuss the following seven cases; elastic, thermal, odd, autonomous three-sphere microswimmers; two interacting ones; and those in viscoelastic and structured fluids. The well-known Purcell's scallop theorem can be generalized for stochastic three-sphere microswimmers and also for the locomotion in viscoelastic and structured fluids.

I. INTRODUCTION

Microswimmers are tiny objects moving in fluids, such as sperm cells or motile bacteria, that swim in a fluid and are expected to be relevant to microfluidics and microsystems [1]. By transforming chemical energy into mechanical work, microswimmers change their shapes and move in viscous environments. The fluid forces acting on the length scale of microswimmers are governed by the effect of viscous dissipation. According to Purcell's scallop theorem, reciprocal body motion cannot be used for locomotion in a Newtonian fluid [2, 3]. As one of the simplest models exhibiting non-reciprocal body motion, Najafi and Golestanian proposed a model of a three-sphere microswimmer [4, 5], in which three in-line spheres are linked by two arms of varying lengths. This model is suitable for analytical studies because the tensorial structure of the fluid motion can be neglected in its translational motion. Later, such a three-sphere microswimmer has been experimentally realized [6–8].

Owing to its simplicity and flexibility, the three-sphere model has been extended and generalized in different ways. For example, the two arms in the original model can be replaced by two elastic springs with time-dependent natural lengths [9–12]. Such an elastic three-sphere microswimmer can include the effects of thermal fluctuations acting on each sphere [13–15]. Then, Purcell's scallop theorem for a deterministic microswimmer, whose deformation is prescribed, can be generalized for a stochastic three-sphere microswimmer in the framework of non-equilibrium statistical mechanics. Using the concept of microrheology [16–18], on the other hand, one can also discuss the locomotion of a three-sphere microswimmer in viscoelastic fluids or structured fluids [19–21]. In this review article, we focus on the three-sphere microswimmer and give an overview of its various extensions that have been developed by the present authors and their

collaborators. Notice that a comprehensive review of three-sphere microswimmers is not intended in this paper.

In Sect. II, we first describe the original three-sphere swimmer proposed by Najafi and Golestanian [4, 5]. In Sect. III, we discuss an elastic three-sphere swimmer, in which the spheres are connected by two springs with time-dependent natural lengths [11]. In Sect. IV, we consider the locomotion of a stochastic microswimmer, in which the three spheres have different temperatures [13]. In Sect. V, we explain a three-sphere microswimmer, in which the spheres are connected by springs that exhibit odd elasticity [14, 15]. In Sect. VI, we propose an autonomous three-sphere microswimmer that can determine the velocity by itself in the steady state [22]. In Sect. VII, we mention the hydrodynamic interaction between two elastic three-sphere microswimmers [23]. In Sect. VIII, we propose a new swimming mechanism for a three-sphere microswimmer in a viscoelastic fluid [19, 20]. In Sect. IX, we further investigate the effects of the intermediate structures of the surrounding viscoelastic fluid on the locomotion of a three-sphere microswimmer [21]. In the final section, we shall provide a brief outlook on the other possible extensions of three-sphere microswimmers.

II. NAJAFI-GOLESTANIAN THREE-SPHERE MICROSWIMMER

In this section, we shall first review the three-sphere microswimmer that was originally proposed by Najafi and Golestanian [4] and later discussed in more detail by Golestanian and Ajdari [5]. Consider a three-sphere microswimmer, in which the positions of the three spheres are given by x_i ($i = 1, 2, 3$) in a one-dimensional coordinate system as shown in Fig. 1(a). One can assume $x_1 < x_2 < x_3$ without loss of generality. Although the size of the three spheres can be different in general [24, 25], we mainly discuss the equal-size case of radius a as it is sufficient to describe the essential swimming mechanism. The three spheres are connected by two arms of lengths L_α ($\alpha = A, B$) that can vary in time. Along the swim-

* komura@wiucas.ac.cn

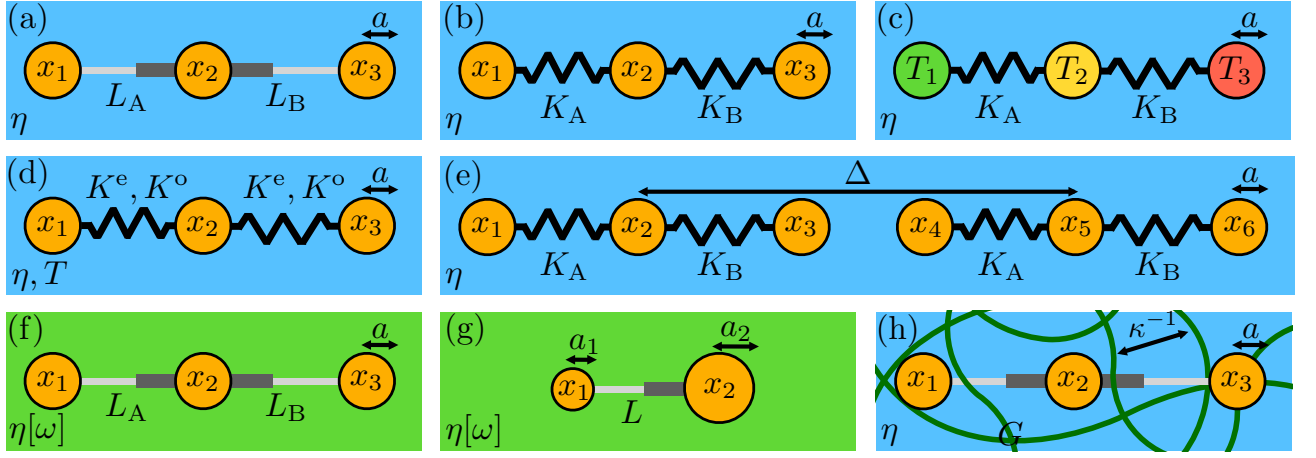


FIG. 1. (Color online) (a) Najafi-Golestanian three-sphere microswimmer model (see Sect. II). Three identical spheres of radius a are connected by two arms of lengths L_A and L_B that undergo prescribed cyclic motions. The positions of the spheres are denoted by x_1 , x_2 , and x_3 in a one-dimensional coordinate system. Such a microswimmer is embedded in a viscous fluid characterized by a constant shear viscosity η . Throughout the paper, we use Roman subscripts $i, j = 1, 2, 3$ for the spheres and Greek subscripts $\alpha, \beta = A, B$ for the arms or the springs. (b) Elastic three-sphere microswimmer in a viscous fluid (see Sect. III). Three spheres are connected by two harmonic springs with elastic constants K_A and K_B . The natural lengths of the springs, denoted by ℓ_A and ℓ_B , undergo prescribed cyclic changes. (c) Thermal three-sphere microswimmer in a viscous fluid (see Sect. IV). Three spheres are connected by two harmonic springs as in (b). In this model, the three spheres are in equilibrium with independent heat baths having different temperatures T_1 , T_2 , and T_3 . Heat transfer between different spheres causes the locomotion of the microswimmer. (d) Odd three-sphere microswimmer in a viscous fluid having temperature T (see Sect. V). Three spheres are connected by two springs with both even elastic constant K^e and odd elastic constant K^o . (The elastic constant K_α in (b) and (c) corresponds to even elasticity.) In this model, odd elasticity causes the non-reciprocal interaction between the two springs. (e) Two interacting elastic three-sphere microswimmers in a viscous fluid (see Sect. VII). The positions of the three spheres in the left (L) swimmer are denoted by x_1 , x_2 , and x_3 , while those in the right (R) swimmer are denoted by x_4 , x_5 , and x_6 . The distance between the two swimmers is defined by $\Delta = x_5 - x_2$. (f) Najafi-Golestanian three-sphere microswimmer in a viscoelastic fluid characterized by a frequency-dependent complex shear viscosity $\eta[\omega]$ (see Sect. VIII). The average velocity has both viscous and elastic contributions indicating the generalization of the scallop theorem for viscoelastic fluids. (g) Asymmetric two-sphere microswimmer in a viscoelastic fluid (see Sect. VIII). Two spheres having different radii a_1 and a_2 ($a_1 < a_2$) are connected by an arm of length L . Since there is only one degree of freedom, any periodic arm motion is reciprocal rather than non-reciprocal. The average velocity of such a two-sphere microswimmer is nonzero. (h) Najafi-Golestanian three-sphere microswimmer in a structured fluid that has intermediate mesoscopic structures (see Sect. IX). Within the two-fluid model, a polymer gel consists of an elastic network characterized by a shear modulus G and a viscous fluid characterized by a viscosity η . Then the viscoelastic time scale is given by $\tau_v = \eta/G$. On the other hand, the elastic and fluid components are coupled to each other through mutual friction. Such friction introduces a characteristic length scale κ^{-1} corresponding to the polymer mesh size. The swimmer sizes (a and ℓ) compete with the characteristic length scale κ^{-1} .

mer axis, each sphere exerts a force f_i on (and experiences a force $-f_i$ from) the fluid having a shear viscosity η . Because we are interested in autonomous net swimming, f_i should satisfy the force-free condition, i.e., $f_1 + f_2 + f_3 = 0$.

For $a/L_\alpha \ll 1$, the equations of motion for each sphere can be written as

$$\dot{x}_i = M_{ij} f_j, \quad (1)$$

where the dot indicates the time derivative, $\dot{x}_i = dx_i/dt$, and M_{ij} is the mobility coefficient matrix describing the hydrodynamic interactions. The summation over repeated indices (i, j and α, β) is assumed throughout this paper. When the spheres are considerably far from each other ($a \ll |x_i - x_j|$), M_{ij} can be approximated as [26]

$$M_{ij} = \begin{cases} 1/(6\pi\eta a) & i = j, \\ 1/(4\pi\eta|x_i - x_j|) & i \neq j. \end{cases} \quad (2)$$

In the above, the case of $i = j$ corresponds to the Stokes mo-

bility, whereas the case of $i \neq j$ describes the hydrodynamic interaction due to the Oseen tensor. However, the tensorial structure of the Oseen tensor does not play a role in the present one-dimensional setup. The total instantaneous velocity of the microswimmer is simply given by $V = (\dot{x}_1 + \dot{x}_2 + \dot{x}_3)/3$.

One way to close the above equations is to prescribe the motion of the two arms. In other words, the arm lengths L_α are known functions of time and they should satisfy the following relations:

$$L_A(t) = x_2(t) - x_1(t), \quad L_B(t) = x_3(t) - x_2(t). \quad (3)$$

Then the total velocity can be obtained in terms of the arm lengths as [5]

$$V = \frac{a}{6} \left[\frac{\dot{L}_B - \dot{L}_A}{L_A + L_B} + 2 \left(\frac{\dot{L}_A}{L_B} - \frac{\dot{L}_B}{L_A} \right) \right]. \quad (4)$$

For relatively small deformations, we can define the small displacements of the arms with respect to the average arm length

ℓ as

$$u_A(t) = x_2(t) - x_1(t) - \ell, \quad u_B(t) = x_3(t) - x_2(t) - \ell, \quad (5)$$

where the condition $u_\alpha/\ell \ll 1$ is assumed. These small displacements are related to the sphere velocities as $\dot{u}_A = \dot{x}_2 - \dot{x}_1$ and $\dot{u}_B = \dot{x}_3 - \dot{x}_2$. Then, up to the leading order in u_α/ℓ , the average swimming velocity can be generally written as [5]

$$\bar{V} = \frac{7a}{24\ell^2} \overline{(u_A \dot{u}_B - \dot{u}_A u_B)}, \quad (6)$$

where the averaging, indicated by the bar, is performed by time integration in a full cycle. The above expression indicates that the average velocity is determined by the area enclosed by the orbit of periodic motion in the configuration space [27, 28]. Hence, Eq. (6) can be understood as the mathematical expression of the scallop theorem as long as the prescribed cyclic deformation is deterministic [2, 3].

As an example, let us consider the following harmonic deformations of the two arms

$$u_A(t) = d_A \cos(\Omega t), \quad u_B(t) = d_B \cos(\Omega t - \phi), \quad (7)$$

where d_α is the amplitude, Ω is the common frequency, and ϕ is the phase difference between the two arms. The average swimming velocity in Eq. (6) now reads

$$\bar{V} = \frac{7ad_A d_B \Omega}{24\ell^2} \sin \phi, \quad (8)$$

which is proportional to Ω . This result clearly shows that \bar{V} is nonzero when $\phi \neq 0, \pi$ for which the arm motion is non-reciprocal. The swimming direction is determined by the sign of $\sin \phi$, and the maximum velocity is obtained when the phase difference is $\phi = \pm\pi/2$. We also remind that \bar{V} in Eq. (8) does not depend on the viscosity η because we have prescribed the motion of the two arms. This situation will be modified in the models discussed later.

III. ELASTIC THREE-SPHERE MICROSWMIMER

In this section, we discuss the first generalization of a three-sphere microswimmer, in which the spheres are connected by two harmonic springs, i.e., an elastic three-sphere microswimmer [11]. In this model, the natural length of each spring depends on time and is assumed to undergo a prescribed cyclic change. Introducing harmonic springs between the spheres leads to an intrinsic time scale of an elastic microswimmer characterizing its internal relaxation dynamics.

As schematically shown in Fig. 1(b), the present model consists of three hard spheres connected by two harmonic springs A and B with spring constants K_A and K_B , respectively. We assume that the natural lengths of these springs, denoted by $\ell_A(t)$ and $\ell_B(t)$, undergo cyclic time-dependent change. Since the energy of an elastic microswimmer is given by

$$E = \frac{K_A}{2} (x_2 - x_1 - \ell_A)^2 + \frac{K_B}{2} (x_3 - x_2 - \ell_B)^2, \quad (9)$$

the three forces $f_i = -\partial E/\partial x_i$ in Eq. (1) read

$$f_1 = K_A(x_2 - x_1 - \ell_A), \quad (10)$$

$$f_2 = -K_A(x_2 - x_1 - \ell_A) + K_B(x_3 - x_2 - \ell_B), \quad (11)$$

$$f_3 = -K_B(x_3 - x_2 - \ell_B). \quad (12)$$

Notice that the force-free condition, $f_1 + f_2 + f_3 = 0$, is automatically satisfied in this model.

Next, we assume that the two natural lengths of the springs undergo the following periodic changes:

$$\ell_A(t) = \ell + d_A \cos(\Omega t), \quad \ell_B(t) = \ell + d_B \cos(\Omega t - \phi). \quad (13)$$

Here, ℓ is the constant natural length, d_α is the amplitude of the oscillatory change, Ω is the common frequency, and ϕ is the phase difference between the two cyclic changes. It is convenient to introduce the characteristic time scale $\tau = 6\pi\eta a/K_A$ and define the scaled frequency by $\hat{\Omega} = \Omega\tau$. We also denote the ratio between the two spring constants by $\lambda = K_B/K_A$.

Similar to Eq. (5), we define the spring extensions u_α relative to ℓ . Then, by using Eq. (6), we obtain the average velocity up to the lowest-order terms as

$$\bar{V} = \frac{7ad_A d_B}{24\ell^2\tau} G_1(\hat{\Omega}; \lambda) \sin \phi + \frac{7(1-\lambda)ad_A d_B}{12\ell^2\tau} G_2(\hat{\Omega}; \lambda) \cos \phi + \frac{7a(d_A^2 - d_B^2\lambda)}{24\ell^2\tau} G_2(\hat{\Omega}; \lambda), \quad (14)$$

where the two scaling functions are given by

$$G_1(\hat{\Omega}; \lambda) = \frac{3\lambda\hat{\Omega}(3\lambda + \hat{\Omega}^2)}{9\lambda^2 + 2(2 + \lambda + 2\lambda^2)\hat{\Omega}^2 + \hat{\Omega}^4}, \quad (15)$$

$$G_2(\hat{\Omega}; \lambda) = \frac{3\lambda\hat{\Omega}^2}{9\lambda^2 + 2(2 + \lambda + 2\lambda^2)\hat{\Omega}^2 + \hat{\Omega}^4}. \quad (16)$$

In Fig. 2, we plot the above scaling functions as functions of $\hat{\Omega}$ for $\lambda = 0.1, 1$ and 10 . Notice, however, that the cases $\lambda = 0.1$ and 10 are essentially equivalent because we can always exchange the springs A and B, whereas we have defined the relaxation time τ by using K_A (and not K_B).

For the symmetric case when $\lambda = 1$ and $d_A = d_B = d$, only the first term in Eq. (14) remains. In this case, we have

$$\bar{V} = \frac{7ad^2}{24\ell^2\tau} \frac{3\hat{\Omega}(3 + \hat{\Omega}^2)}{9 + 10\hat{\Omega}^2 + \hat{\Omega}^4} \sin \phi. \quad (17)$$

In the small-frequency limit of $\hat{\Omega} \ll 1$, the average velocity increases as $\bar{V} \sim \Omega$ and coincides with Eq. (8). This is because small $\hat{\Omega}$ corresponds to large K_A and the springs behave as rigid arms. In the opposite large-frequency limit of $\hat{\Omega} \gg 1$, on the other hand, the average velocity decreases as $\bar{V} \sim \Omega^{-1}$ as Ω is increased. When K_A is small, it takes time for the spring to relax to its natural length, which delays the mechanical response. The crossover frequency between the above two regimes is given by $\hat{\Omega}^* \approx 1$.

When $\lambda \neq 1$, on the other hand, the second term in Eq. (14) is present even if $\phi = 0$. The third term is also present when $d_A^2 \neq d_B^2\lambda$, regardless of the ϕ -value. In contrast to the

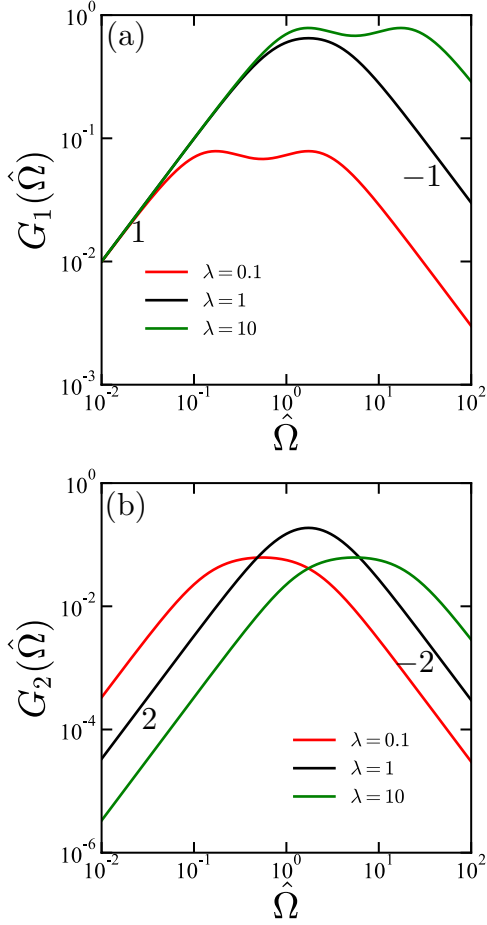


FIG. 2. (Color online) Plots of the scaling functions (a) $G_1(\hat{\Omega}; \lambda)$ and (b) $G_2(\hat{\Omega}; \lambda)$ defined in Eqs. (15) and (16), respectively, as functions of $\hat{\Omega} = \Omega\tau$ ($\tau = 6\pi\eta a/K_A$) for $\lambda = K_B/K_A = 0.1, 1$, and 10 . The numbers indicate the slope representing the exponent of the power-law behaviors. Reprinted from Ref. [11]. © 2017 The Physical Society of Japan.

first term representing the non-reciprocal arm motion, both the second and third terms reflect the structural asymmetry of an elastic three-sphere microswimmer. The frequency dependence of the second and third terms, represented by $G_2(\hat{\Omega}, \lambda)$, differs from that of the first term, represented by $G_1(\hat{\Omega}, \lambda)$. From Eq. (16), we see that \bar{V} due to the second and third terms increases as $\bar{V} \sim \Omega^2$ for $\hat{\Omega} \ll 1$, whereas it decreases as $\bar{V} \sim \Omega^{-2}$ for $\hat{\Omega} \gg 1$.

In general, the overall swimming velocity depends on various structural parameters and exhibits a complex frequency dependence. For example, $G_1(\hat{\Omega}, \lambda)$ in Fig. 2(a) exhibits a non-monotonic frequency dependence (two maxima) for $\lambda = 0.1$ and 10 . On the other hand, an important common feature for all the terms in Eq. (14) is that \bar{V} decreases for large $\hat{\Omega}$, which is a characteristic feature of an elastic three-sphere microswimmer.

IV. THERMAL THREE-SPHERE MICROSWIMMER

Extending the model of an elastic three-sphere microswimmer, we propose a different locomotion mechanism that is purely induced by thermal fluctuations [13]. Here, the key assumption is that the three spheres are in equilibrium with independent heat baths at different temperatures. Then, the heat transfer occurs from a hotter sphere to a colder one, driving the whole system out of equilibrium. Since this model is similar to a class of thermal ratchet models, the suggested mechanism can be relevant to the non-equilibrium dynamics of proteins and enzymes in biological systems [29].

As shown in Fig. 1(c), we consider an elastic three-sphere microswimmer, in which the three spheres are in equilibrium with independent heat baths having temperatures T_i . When these temperatures are different, the system is driven out of equilibrium because a heat flux is generated from a hotter sphere to a colder one. In the presence of thermal fluctuations, the equations of motion of the three spheres can be written as [30]

$$\dot{x}_i = M_{ij}f_j + \xi_i, \quad (18)$$

where the mobility matrix M_{ij} is given by Eq. (2) and the forces f_i are given by Eqs. (10)-(12) as before. The additional terms describing the white-noise sources $\xi_i(t)$ have zero mean, i.e., $\langle \xi_i(t) \rangle = 0$, and their correlations satisfy

$$\langle \xi_i(t)\xi_j(t') \rangle = 2D_{ij}\delta(t-t'), \quad (19)$$

where $\langle \dots \rangle$ indicates the ensemble average, namely, the average for many equivalent systems. In the above, D_{ij} is the mutual diffusion coefficient given by

$$D_{ij} = \begin{cases} k_B T_i / (6\pi\eta a) & i = j, \\ k_B \Theta(T_i, T_j) / (4\pi\eta |x_i - x_j|) & i \neq j, \end{cases} \quad (20)$$

where k_B is the Boltzmann constant and $\Theta(T_i, T_j)$ is a function of T_i and T_j . The relevant effective temperature can be the mobility-weighted average [31], which in the present case is simply given by $\Theta(T_i, T_j) = (T_i + T_j)/2$ because all the spheres have the same size. However, its explicit functional form is not needed here, and we only require that Θ should satisfy an appropriate fluctuation-dissipation theorem in thermal equilibrium. This is allowed because we only consider the limit of $a \ll \ell$.

The above stochastic equations can be solved in the Fourier domain. Assuming $u_\alpha \ll \ell$ and $a \ll \ell$, we obtain the lowest-order average velocity as [13]

$$\langle V \rangle = \frac{k_B}{144\pi\eta\ell^2(1+\lambda)} [(2-5\lambda)T_1 - 7(1-\lambda)T_2 + (5-2\lambda)T_3], \quad (21)$$

where $\lambda = K_B/K_A$ as before. When the three temperatures are identical ($T_1 = T_2 = T_3$), the velocity vanishes identically, $\langle V \rangle = 0$. This indicates that a thermal three-sphere microswimmer can acquire a finite velocity owing to the temperature difference among the spheres.

When the springs are symmetric and $\lambda = 1$, Eq. (21) reduces to

$$\langle V \rangle = \frac{k_B(T_3 - T_1)}{96\pi\eta\ell^2}, \quad (22)$$

which is proportional to the temperature difference $T_3 - T_1$. Since we have assumed $x_1 < x_2 < x_3$, the swimming direction is from a colder sphere to a hotter one ($\langle V \rangle > 0$) when $T_3 > T_1$ and vice versa. It is also remarkable that Eq. (22) does not depend on the temperature T_2 of the middle sphere. Hence $\langle V \rangle = 0$ when $T_1 = T_3$ even though T_1 and T_3 are different from T_2 . However, the presence of the middle sphere is essential for directional locomotion because the hydrodynamic interactions among the three spheres are responsible for the motion.

The analytically obtained velocity in Eq. (21) can be related to the heat flows in the steady state. Following Ref. [32] and retaining up to the lowest-order terms, we obtain the average heat gain per unit time for each sphere as

$$\langle \dot{Q}_1 \rangle = \frac{k_B}{6\tau(1+\lambda)} [(3+2\lambda)T_1 - (3+\lambda)T_2 - \lambda T_3], \quad (23)$$

$$\langle \dot{Q}_2 \rangle = \frac{k_B}{6\tau(1+\lambda)} [-(3+\lambda)T_1 + (3+2\lambda+3\lambda^2)T_2 - (\lambda+3\lambda^2)T_3], \quad (24)$$

$$\langle \dot{Q}_3 \rangle = \frac{k_B}{6\tau(1+\lambda)} [-\lambda T_1 - (\lambda+3\lambda^2)T_2 + (2\lambda+3\lambda^2)T_3], \quad (25)$$

which all vanish when $T_1 = T_2 = T_3$. Notice that the above heat flows also satisfy $\langle \dot{Q}_1 \rangle + \langle \dot{Q}_2 \rangle + \langle \dot{Q}_3 \rangle = 0$. Assuming a linear relationship between the average velocity in Eq. (21) and the heat flows in Eqs. (23)-(25), we obtain an alternative expression for the velocity:

$$\langle V \rangle = \frac{a}{8K_A\ell^2} \left[\frac{3-5\lambda}{1+\lambda} \langle \dot{Q}_1 \rangle + \frac{5-3\lambda}{\lambda(1+\lambda)} \langle \dot{Q}_3 \rangle \right]. \quad (26)$$

For the symmetric case of $\lambda = 1$ corresponding to Eq. (22), the above expression reduces to

$$\langle V \rangle = \frac{a}{8K_A\ell^2} [\langle \dot{Q}_3 \rangle - \langle \dot{Q}_1 \rangle]. \quad (27)$$

This relation indicates that the net heat flow between the first and third spheres determines the average velocity.

Previously, Yang *et al.* performed hydrodynamic simulations of a self-thermophoretic Janus particle [33] and they reproduced the experimental observation by Jiang *et al.* [34]. The above thermal three-sphere microswimmer is different because thermal fluctuations of internal degrees of freedom cause locomotion. We also note from Eq. (21) that $\langle V \rangle$ is nonzero for symmetric temperatures $T_1 = T_3 \neq T_2$ as long as the structural asymmetry exists ($\lambda \neq 0$), which cannot be realized for a thermophoretic Janus particle.

V. ODD THREE-SPHERE MICROSWMIMER

Recently, Scheibner *et al.* introduced the concept of odd elasticity that arises from non-reciprocal interactions in active

systems [35, 36]. The odd part of the elastic constant matrix quantifies the amount of work extracted along quasistatic deformation cycles. In this section, we discuss another type of thermally driven microswimmer, in which the three spheres are connected by odd springs [14, 15].

As shown in Fig. 1(d), consider an elastic three-sphere microswimmer, in which the three spheres are connected by two identical springs that exhibit both even and odd elasticity. Then, the forces F_A and F_B conjugate to the spring extensions u_A and u_B [see Eq. (5)], respectively, are given by $F_\alpha = -K_{\alpha\beta}u_\beta$. For an odd spring, the elastic constant matrix $K_{\alpha\beta}$ is given by [37–40]

$$K_{\alpha\beta} = K^e\delta_{\alpha\beta} + K^o\epsilon_{\alpha\beta}. \quad (28)$$

Here, K^e and K^o are the even and odd elastic constants, respectively, in the two-dimensional configuration space spanned by u_A and u_B , $\delta_{\alpha\beta}$ is the Kronecker delta, and $\epsilon_{\alpha\beta}$ is the two-dimensional Levi-Civita tensor with $\epsilon_{AA} = \epsilon_{BB} = 0$ and $\epsilon_{AB} = -\epsilon_{BA} = 1$. (The spring constants K_A and K_B in Sect. III correspond to even elastic constants.) The presence of the odd elasticity K^o in Eq. (28) reflects the non-reciprocal interaction between the two springs such that u_A and u_B influence each other in a different way. The forces f_i acting on each sphere are given by $f_1 = -F_A$, $f_2 = F_A - F_B$, and $f_3 = F_B$.

Such an odd microswimmer is immersed in a fluid with a shear viscosity of η and temperature T . Similar to the previous stochastic model, the equations of motion for each sphere are given by Eq. (18). In the current model, the Gaussian white-noise sources ξ_i also have zero mean $\langle \xi_i(t) \rangle = 0$, and their correlations satisfy the following fluctuation-dissipation theorem:

$$\langle \xi_i(t)\xi_j(t') \rangle = 2k_B T M_{ij} \delta(t-t'), \quad (29)$$

where M_{ij} is given by Eq. (2).

The equal-time correlation functions can be obtained from the reduced Langevin equations for $\dot{u}_A = \dot{x}_2 - \dot{x}_1$ and $\dot{u}_B = \dot{x}_3 - \dot{x}_2$ as

$$\dot{u}_\alpha = \Gamma_{\alpha\beta}u_\beta + \Xi_\alpha. \quad (30)$$

In the above, $\Gamma_{\alpha\beta}$ and Ξ_α are

$$\mathbf{\Gamma} = -\frac{1}{\tau} \begin{pmatrix} 2+\nu & -1+2\nu \\ -1-2\nu & 2-\nu \end{pmatrix}, \quad \mathbf{\Xi} = \begin{pmatrix} \xi_2 - \xi_1 \\ \xi_3 - \xi_2 \end{pmatrix}, \quad (31)$$

where $\tau = 6\pi\eta a/K^e$ and we have introduced the ratio $\nu = K^o/K^e$. Notice that $\Gamma_{\alpha\beta}$ is non-reciprocal, i.e., $\Gamma_{AB} \neq \Gamma_{BA}$ when $\nu \neq 0$. By solving Eq. (30) in the Fourier domain and using Eq. (29), we can calculate the equal-time correlation functions $\langle u_A^2 \rangle$, $\langle u_B^2 \rangle$, and $\langle u_A u_B \rangle$. From these quantities, we obtain the average velocity as

$$\langle V \rangle = \frac{7k_B T \nu}{48\pi\eta\ell^2}. \quad (32)$$

We see here that $\langle V \rangle$ is proportional to the odd elastic constant K^o that can take both positive and negative values.

Next, we discuss the non-equilibrium statistical properties of the odd three-sphere microswimmer [41, 42]. Consider the

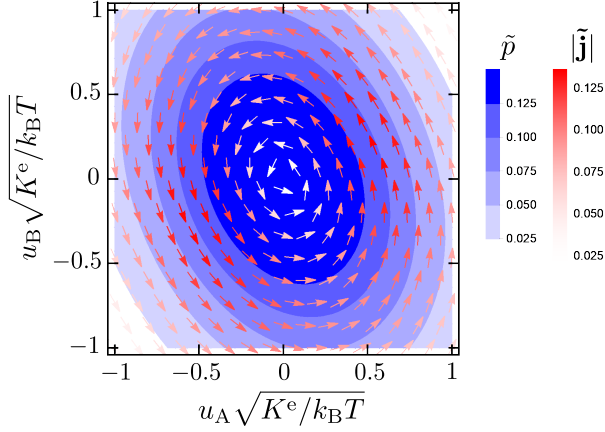


FIG. 3. (Color online) Steady-state scaled probability distribution function $\tilde{p} = p k_B T / K^e$ [see Eq. (35)] and scaled probability flux $\tilde{\mathbf{j}} = \mathbf{j} \tau \sqrt{k_B T / K^e}$ [arrows, see Eq. (33)] ($\tau = 6\pi\eta a / K^e$) in the configuration space spanned by u_A and u_B when $\nu = K^o / K^e = 1$. Reproduced from Ref. [14]. © 2021 K. Yasuda, Y. Hosaka, I. Sou, and S. Komura.

time-dependent probability distribution function $p(u_A, u_B, t)$. The Fokker-Planck equation that corresponds to Eq. (30) can be written as $\dot{p} = -\partial_\alpha j_\alpha$, where $\partial_\alpha = \partial / (\partial u_\alpha)$ and j_α is the probability flux given by [43, 44]

$$j_\alpha = \Gamma_{\alpha\beta} u_\beta p - \mathcal{D}_{\alpha\beta} \partial_\beta p. \quad (33)$$

Here, $\mathcal{D}_{\alpha\beta}$ is the diffusion matrix

$$\mathcal{D} = \frac{k_B T}{6\pi\eta a} \begin{pmatrix} 2 & -1 \\ -1 & 2 \end{pmatrix}, \quad (34)$$

that satisfies the fluctuation-dissipation relation $\langle \Xi_\alpha(t) \Xi_\beta(t') \rangle = 2\mathcal{D}_{\alpha\beta} \delta(t - t')$ because of Eq. (29) [note that $\mathcal{D}_{\alpha\beta}$ is different from D_{ij} in Eqs. (19)].

Owing to the reproductive property of Gaussian distributions, the steady-state probability distribution function that satisfies $\dot{p} = 0$ is given by the following Gaussian function

$$p(u_A, u_B) = \frac{1}{2\pi \sqrt{\det \mathbf{C}}} \exp \left[-\frac{1}{2} (\mathbf{C}^{-1})_{\alpha\beta} u_\alpha u_\beta \right]. \quad (35)$$

Here, $C_{\alpha\beta} = \langle u_\alpha u_\beta \rangle$ is the covariance matrix given by

$$\mathbf{C} = \frac{k_B T}{K^e} \frac{1}{1 + \nu^2} \begin{pmatrix} 1 - \nu/2 + \nu^2 & -\nu^2/2 \\ -\nu^2/2 & 1 + \nu/2 + \nu^2 \end{pmatrix}, \quad (36)$$

and $(\mathbf{C}^{-1})_{\alpha\beta}$ is the inverse matrix of $C_{\alpha\beta}$. Then the determinant of \mathbf{C} becomes

$$\det \mathbf{C} = \left(\frac{k_B T}{K^e} \right)^2 \frac{4 + 7\nu^2 + 3\nu^4}{4(1 + \nu^2)^2}. \quad (37)$$

In Fig. 3, we plot the steady-state probability distribution function [Eq. (35)] and the corresponding probability flux [Eq. (33)] when $\nu = 1$. The probability distribution function

is distorted by the negative correlation ($C_{AB} = C_{BA} \sim -\nu^2/2$) between u_A and u_B . Importantly, one can see a counter-clockwise loop of the probability flux. Such a probability flux becomes clockwise for $\nu < 0$ and vanishes when $\nu = 0$. Generally, the existence of the probability flux loop indicates that the detailed balance is broken in the non-equilibrium steady state [45, 46]. In contrast to the deterministic scallop theorem mentioned in Eq. (6), the presence of the probability flux loop can be regarded as the stochastic scallop theorem that can be applied to thermally driven microswimmers [13–15, 40, 43, 44].

The steady-state probability flux can be conveniently expressed in terms of a frequency matrix $\Omega_{\alpha\beta}$ as $j_\alpha = \Omega_{\alpha\beta} u_\beta p$ [41, 42]. In the current model, the frequency matrix is given by

$$\boldsymbol{\Omega} = \frac{3\nu}{\tau(4 + 3\nu^2)} \begin{pmatrix} -\nu^2 & -2 + \nu - 2\nu^2 \\ 2 + \nu + 2\nu^2 & \nu^2 \end{pmatrix}, \quad (38)$$

which is traceless. Then, the two eigenvalues of $\Omega_{\alpha\beta}$ are given by

$$\gamma = \pm i \frac{3\nu}{\tau(4 + 3\nu^2)} \sqrt{4 + 7\nu^2 + 3\nu^4}. \quad (39)$$

Comparing Eq. (32) with Eqs. (37) and (39), we obtain the following alternative expression for the absolute value of the average velocity:

$$|\langle V \rangle| = \frac{7a}{12\ell^2} \sqrt{\det \mathbf{C}} |\gamma|. \quad (40)$$

Here, $7a/(12\ell^2)$ is the geometrical factor, $\sqrt{\det \mathbf{C}} \sim k_B T / K^e$ is the randomly explored area in the configuration space, and $|\gamma| \sim \tau^{-1}$ is the frequency of the rotational probability flux. The above expression clarifies the physical meaning of the average velocity of an odd three-sphere microswimmer driven by thermal fluctuations.

VI. AUTONOMOUS THREE-SPHERE MICROSWMIMER

In this section, we propose a model of a three-sphere swimmer that can autonomously determine its velocity [22]. To implement such a control mechanism, we introduce a coupling between the two natural lengths of an elastic microswimmer by using the interaction adopted in the Kuramoto model for coupled oscillators [47, 48]. Such a microswimmer acquires a steady-state velocity and a finite phase difference in the long-time limit without any external control.

Consider a symmetric elastic three-sphere microswimmer ($\lambda = 1$), in which the natural lengths of the springs undergo the following cyclic changes in time

$$\ell_A(t) = \ell + d \cos[\theta_A(t)], \quad \ell_B(t) = \ell + d \cos[\theta_B(t)], \quad (41)$$

where $\theta_A(t)$ and $\theta_B(t)$ are the time-dependent phases. Although these motions are the generalization of Eq. (13), the important feature is that $\theta_A(t)$ and $\theta_B(t)$ are affected by the relative positions and the velocities of the three spheres. We

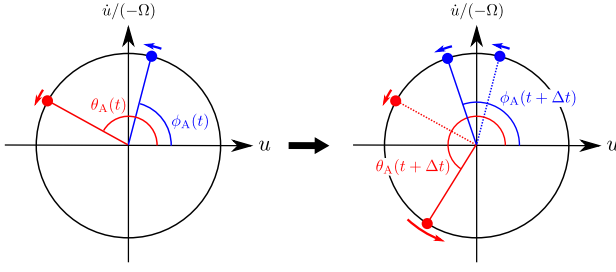


FIG. 4. (Color online) Dynamics of θ_A describing the phase of the natural length [see Eq. (41)] and ϕ_A describing the mechanical phase [see Eq. (44)]. When $\theta_A > \phi_A$ at t , as shown in the left figure, and when $\chi > 0$ in Eq. (42), the velocity $\dot{\theta}_A$ becomes larger at a later time $t + \Delta t$, as shown in the right figure. As a result, the difference between θ_A and ϕ_A also increases at $t + \Delta t$. A similar dynamics occurs also for θ_B and ϕ_B . Reprinted from Ref. [22]. © 2021 Institute of Physics.

employ the following time-evolution equations for $\theta_A(t)$ and $\theta_B(t)$ that describe a synchronization behavior [47, 48]

$$\dot{\theta}_A = \Omega + \chi \sin[\theta_A(t) - \phi_A(t)], \quad (42)$$

$$\dot{\theta}_B = \Omega + \chi \sin[\theta_B(t) - \phi_B(t)], \quad (43)$$

where Ω is the constant frequency, $\chi \geq 0$ is the coupling parameter representing the strength of synchronization, and ϕ_A and ϕ_B are the mechanical phases as explained below.

To discuss the above mechanical phases, we use the spring displacements u_A and u_B defined in Eq. (5). Then the mechanical phases ϕ_A and ϕ_B are introduced by the relative positions and the velocities of the spheres as

$$\cos \phi_A = u_A/U_A, \quad \sin \phi_A = -\dot{u}_A/(\Omega U_A), \quad (44)$$

$$\cos \phi_B = u_B/U_B, \quad \sin \phi_B = -\dot{u}_B/(\Omega U_B), \quad (45)$$

where $U_{A(B)} = [u_{A(B)}^2 + (\dot{u}_{A(B)}/\Omega)^2]^{1/2}$. The above equations complete the model for an autonomous three-sphere microswimmer.

The physical meaning of Eqs. (42) and (43) is that the phase θ_A (θ_B) for the natural length and the mechanical phase ϕ_A (ϕ_B) tend to be different due to the coupling term with χ , as schematically explained in Fig. 4. Since the middle sphere is connected to the other two spheres, this model contains a feedback mechanism that regulates the dynamics of the two natural lengths ℓ_A and ℓ_B . Such a coupling effect in the spring motion gives rise to a non-reciprocal body motion and results in the autonomous locomotion of a microswimmer.

Let us define the time-dependent phase difference between the oscillations in the natural lengths by $\delta(t) = \theta_B(t) - \theta_A(t)$. When $\chi = 0$, the present model reduces to the elastic three-sphere microswimmer discussed in Sect. III. In this limit, we have $\theta_A(t) = \Omega t$ and $\theta_B(t) = \Omega t + \delta_0$, where $\delta_0 = \delta(0)$ is the initial phase difference. Hence, the initial phase difference δ_0 and the frequency Ω fully determine the average velocity of locomotion when $\chi = 0$.

When $\chi > 0$, however, a stable phase difference δ controls the dynamics of a microswimmer irrespective of its initial value δ_0 . Moreover, the transition to a non-reciprocal motion, as well as the average velocity, can be precisely tuned

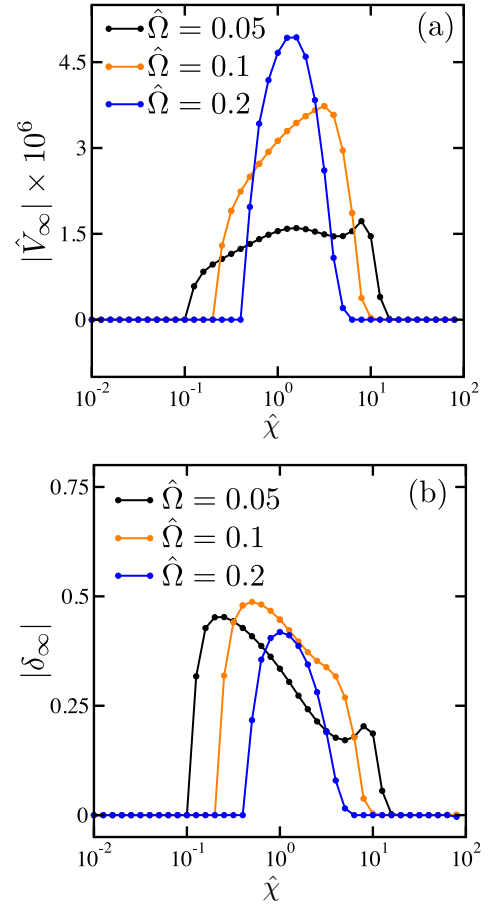


FIG. 5. (Color online) Plots of (a) dimensionless stationary velocity $|\hat{V}_\infty| = |V_\infty \tau / \ell|$ and (b) stationary phase difference $|\delta_\infty|$ as a function of the dimensionless coupling parameter $\hat{\chi} = \chi \tau$ ($\tau = 6\pi\eta a / K_A$). In both plots, the dimensionless frequency is chosen as $\hat{\Omega} = 0.05$ (black), 0.1 (orange), and 0.2 (blue), while $\delta_0 = -\pi/2$ is fixed. There is a lower critical value $\hat{\chi}_c$ above which both $|V_\infty|$ and $|\delta_\infty|$ become nonzero. $|V_\infty|$ and $|\delta_\infty|$ take maximum values at $\hat{\chi}_m > \hat{\chi}_c$, and they vanish for large $\hat{\chi}$. Reprinted from Ref. [22]. © 2021 Institute of Physics.

by χ , and they are not solely fixed by the externally given frequency Ω . In Figs. 5(a) and (b), we plot the numerically obtained steady-state velocity $|V_\infty|$ and the phase difference $|\delta_\infty|$, respectively, as a function of $\hat{\chi} = \chi \tau$ for different frequencies $\hat{\Omega} = \Omega \tau$ ($\tau = 6\pi\eta a / K_A$). When $\hat{\Omega} = 0.1$ (orange), for example, there is a critical value $\hat{\chi}_c \approx 0.2$ above which $|V_\infty|$ and $|\delta_\infty|$ become nonzero. For $\hat{\chi} < \hat{\chi}_c$, on the other hand, both $|V_\infty|$ and $|\delta_\infty|$ vanish. The existence of such a finite critical value $\hat{\chi}_c$ is a nontrivial outcome of the present model. When $\hat{\chi}$ is very large, such as $\hat{\chi} \geq 12.5$ for $\hat{\Omega} = 0.1$, both $|V_\infty|$ and $|\delta_\infty|$ vanish again. Hence autonomous locomotion can be achieved for a finite range of the coupling parameter χ . Such behavior can also be observed for other frequencies $\hat{\Omega}$.

VII. TWO INTERACTING THREE-SPHERE MICROSWIMMERS

Next, we discuss the behaviors of two interacting elastic three-sphere microswimmers in a viscous fluid as shown in Fig. 1(e) [23]. The positions of the three spheres in the left (L) swimmer are denoted by x_1 , x_2 , and x_3 , while those in the right (R) swimmer are denoted by x_4 , x_5 , and x_6 . We consider the situation when $x_1 < x_2 < x_3 \ll x_4 < x_5 < x_6$ is satisfied. The distance between the two swimmers is defined by the positions of the two middle spheres, i.e., $\Delta = x_5 - x_2$.

The equations of motion of each sphere ($i = 1, \dots, 6$) are given by Eq. (1) as before but we do not consider any noise here. We require two force-free conditions for each swimmer, i.e., $f_1 + f_2 + f_3 = 0$ and $f_4 + f_5 + f_6 = 0$. Similar to Eq. (5), we define the four displacements of the springs with respect to the natural length ℓ for the left and right swimmers as

$$u_A^L(t) = x_2(t) - x_1(t) - \ell, \quad u_B^L(t) = x_3(t) - x_2(t) - \ell, \quad (46)$$

$$u_A^R(t) = x_5(t) - x_4(t) - \ell, \quad u_B^R(t) = x_6(t) - x_5(t) - \ell. \quad (47)$$

The average velocities of the left and right swimmers can be calculated by $V^L = (\dot{x}_1 + \dot{x}_2 + \dot{x}_3)/3$ and $V^R = (\dot{x}_4 + \dot{x}_5 + \dot{x}_6)/3$, respectively.

Under the condition that the two swimmers are far from each other and the deformations are small compared with ℓ , i.e., $a \ll u_{A,B}^{L,R} \ll \ell \ll \Delta$, one can perform a perturbative calculation to obtain the average velocities as

$$\begin{aligned} \bar{V}^L &= \frac{7a}{24\ell^2} \overline{(u_A^L \dot{u}_B^L - u_B^L \dot{u}_A^L)} \\ &- \frac{a\ell}{\Delta^3} \overline{(u_A^R \dot{u}_B^R - u_B^R \dot{u}_A^R - u_A^L \dot{u}_A^R - u_A^L \dot{u}_B^R + u_B^L \dot{u}_A^R + u_B^L \dot{u}_B^R)}, \end{aligned} \quad (48)$$

$$\begin{aligned} \bar{V}^R &= \frac{7a}{24\ell^2} \overline{(u_A^R \dot{u}_B^R - u_B^R \dot{u}_A^R)} \\ &- \frac{a\ell}{\Delta^3} \overline{(u_A^L \dot{u}_B^L - u_B^L \dot{u}_A^L - u_A^R \dot{u}_A^L - u_A^R \dot{u}_B^L + u_B^R \dot{u}_A^L + u_B^R \dot{u}_B^L)}. \end{aligned} \quad (49)$$

Here we have kept only up to second-order terms in $u_{A,B}^{L,R}$, because of the condition $u_{A,B}^{L,R}/\ell \ll \ell/\Delta$ [49]. The first terms on the right-hand side of the above equations represent the average swimming velocity of a single three-sphere swimmer, as we have obtained in Eq. (6).

The second terms on the right-hand side of Eqs. (48) and (49) are due to the hydrodynamic interaction between the two swimmers. These correction terms decay as $(\ell/\Delta)^3$ with increasing distance because they result from force quadrupoles rather than force dipoles. The correction terms $(u_A^R \dot{u}_B^R - u_B^R \dot{u}_A^R)$ in V^L and $(u_A^L \dot{u}_B^L - u_B^L \dot{u}_A^L)$ in V^R are both passive terms because they correspond to the swimming of only the second swimmer. The other correction terms are due to the simultaneous motion of the two swimmers and hence are called active terms [50, 51].

More detailed analysis of Eqs. (48) and (49) reveals that the mean of the two average velocities $(\bar{V}^L + \bar{V}^R)/2$ is always smaller than that of a single elastic swimmer [23]. On the other hand, the velocity difference $\bar{V}^L - \bar{V}^R$ depends on the

relative phase difference between the two elastic swimmers. As a result, the swimming state of two elastic swimmers can be either bound or unbound depending on the relative phase difference [23]. A more extended study on the interaction between two elastic microswimmers is given in Ref. [52].

VIII. THREE-SPHERE MICROSWIMMER IN A VISCOELASTIC FLUID

For microswimmers moving in soft materials, the surrounding fluid is not necessarily purely viscous but viscoelastic. Several studies have discussed the swimming behaviors of microswimmers in different types of viscoelastic fluids [53–60]. In this section, we discuss a three-sphere microswimmer in a general viscoelastic medium [19, 20]. As shown in Fig. 1(f), we consider the original three-sphere microswimmer as in Sect. II.

The equation that describes the hydrodynamics of a low-Reynolds-number flow in a viscoelastic medium is given by the following generalized Stokes equation [61]:

$$\int_{-\infty}^t dt' \eta(t-t') \nabla^2 \mathbf{v}(\mathbf{r}, t') - \nabla P(\mathbf{r}, t) = 0. \quad (50)$$

Here $\eta(t)$ is the time-dependent shear viscosity, \mathbf{v} is the velocity field, P is the pressure, and \mathbf{r} stands for a three-dimensional positional vector. The above equation is further subjected to the incompressibility condition, $\nabla \cdot \mathbf{v} = 0$.

In the context of microrheology [16–18], one uses a linear relation between the time-dependent force $F(t)$ acting on a sphere of radius a and its time-dependent velocity $V(t)$ in the Fourier domain. Such a linear response is written as $V(\omega) = \mu[\omega]F(\omega)$, where $V(\omega) = \int_{-\infty}^{\infty} dt V(t)e^{-i\omega t}$, for example, and the frequency-dependent self-mobility is given by $\mu[\omega] = (6\pi\eta[\omega]a)^{-1}$, where $\eta[\omega] = \int_0^{\infty} dt \eta(t)e^{-i\omega t}$ [17]. Similarly, the force $F_j(t)$ acting on the j -th sphere at x_j and the induced velocity $V_i(t)$ of the i -th sphere at x_i ($i \neq j$) are related by $V_i(\omega) = M[\omega]F_j(\omega)$, where $M[\omega] = (4\pi\eta[\omega]r)^{-1}$ is the frequency-dependent coupling mobility and $r = |x_i - x_j|$ [62]. By using these relations, the equations of motion for a three-sphere microswimmer in a viscoelastic fluid can be written similarly to Eq. (1) in the Fourier domain.

We assume Eq. (7) for the prescribed motion of the two arms. Up to the lowest order terms in a , the average swimming velocity over one cycle of motion is obtained as [19, 20]

$$\bar{V} = \frac{7ad_A d_B \Omega}{24\ell^2} \frac{\eta'[\Omega]}{\eta_0} \sin \phi - \frac{5a(d_A^2 - d_B^2)\Omega}{48\ell^2} \frac{\eta''[\Omega]}{\eta_0}, \quad (51)$$

where $\eta'[\Omega]$ and $\eta''[\Omega]$ are the real and imaginary parts of the complex shear viscosity, respectively, and $\eta_0 = \eta[\Omega \rightarrow 0]$ is the constant zero-frequency viscosity. The first term can be regarded as the viscous contribution because it includes the real part $\eta'[\Omega]$, and is present only if the arm motion is non-reciprocal, i.e., $\phi \neq 0, \pi$. The second term, on the other hand, corresponds to the elastic contribution because it contains the imaginary part $\eta''[\Omega]$, and it exists only when the structural symmetry of the swimmer is broken, i.e., $d_A \neq d_B$. Due to the

presence of the second term, Purcell's scallop theorem can be generalized for viscoelastic fluids. For a purely Newtonian fluid ($\eta[\Omega] = \eta_0$), the second term vanishes, and the first term coincides with Eq. (8).

As an illustration of the above result, we assume that the surrounding viscoelastic medium is described by the Maxwell model. In this case, the frequency-dependent viscosity can be written as

$$\eta[\omega] = \eta_0 \frac{1 - i\omega\tau_M}{1 + \omega^2\tau_M^2}, \quad (52)$$

where τ_M is the characteristic time scale. Such a medium is viscous for $\omega\tau_M \ll 1$, while it becomes elastic for $\omega\tau_M \gg 1$. Then, the average swimming velocity in Eq. (51) becomes

$$\bar{V} = \frac{7ad_A d_B \Omega}{24\ell^2} \frac{1}{1 + \Omega^2\tau_M^2} \sin\phi + \frac{5a(d_A^2 - d_B^2)\Omega}{48\ell^2} \frac{\Omega\tau_M}{1 + \Omega^2\tau_M^2}. \quad (53)$$

The first viscous term increases as $\bar{V} \sim \Omega$ for $\Omega\tau_M \ll 1$, while it decreases as $\bar{V} \sim \Omega^{-1}$ for $\Omega\tau_M \gg 1$. On the other hand, the second elastic term increases as $\bar{V} \sim \Omega^2$ for $\Omega\tau_M \ll 1$, and it approaches a constant value for $\Omega\tau_M \gg 1$. In Figs. 6(a) and (b), we plot these viscous and elastic contributions to the average velocity \bar{V} , respectively, as a function of $\Omega\tau_M$. We note here the similarity between Figs. 2(a) and 6(a) showing the decrease of the velocity in the high-frequency regime.

In the rest of this section, we mention two other situations; (i) a three-sphere microswimmer [see Fig. 1(f)] and (ii) a two-sphere microswimmer [see Fig. 1(g)], in which the microswimmer undergoes a reciprocal (rather than non-reciprocal) motion in a viscoelastic fluid [20]. In the first case, we consider a three-sphere microswimmer whose two arms are subjected to different frequencies. In particular, we consider the following time dependencies of the two arms:

$$L_A(t) = \ell + d \cos(\Omega t), \quad L_B(t) = \ell + d \cos(2\Omega t), \quad (54)$$

where the frequencies of L_A and L_B are Ω and 2Ω , respectively, while the amplitude d is taken to be the same. (In general, the frequency of L_B can be $n\Omega$ where n is an integer.) Since the arm frequencies are different, a phase shift does not play any role, and the overall arm motion turns out to be reciprocal. Nevertheless, the average velocity is obtained as

$$\bar{V} = \frac{5ad^2\Omega}{48\ell^2\eta_0} (2\eta''[2\Omega] - \eta''[\Omega]), \quad (55)$$

where only the imaginary parts of the complex shear viscosity appear. The above result indicates that a reciprocal microswimmer can move as long as $\eta''[\Omega] \neq 2\eta''[2\Omega]$.

In the second case, we consider a two-sphere microswimmer consisting of two spheres having different sizes a_1 and a_2 , as shown in Fig. 1(g) [20]. These two spheres are connected by a single arm which undergoes the periodic motion $L(t) = \ell + d \cos(\Omega t)$. Since there is only one arm, it is obvious that any periodic arm motion is inevitably reciprocal. Calculating the total swimming velocity by $V = (\dot{x}_1 + \dot{x}_2)/2$, we

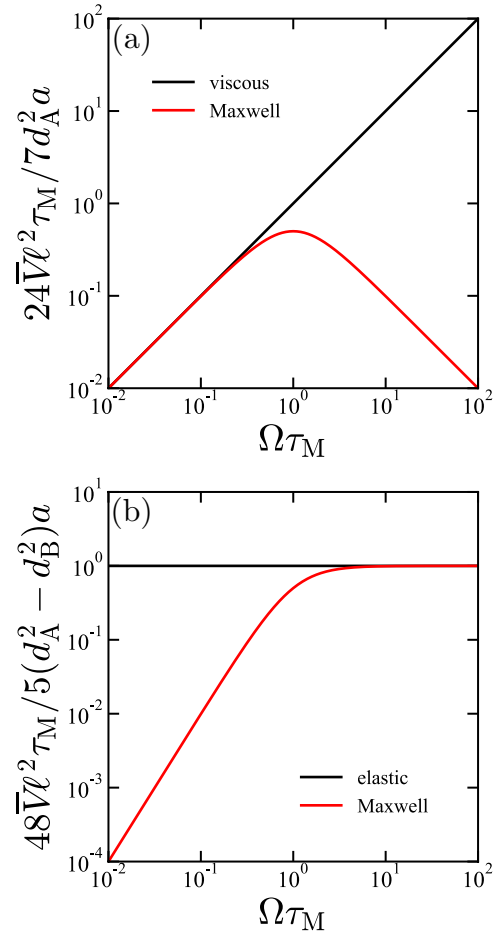


FIG. 6. (Color online) Average swimming velocity \bar{V} as a function of $\Omega\tau_M$ for a three-sphere microswimmer in a viscoelastic Maxwell fluid [see Eq. (52)]. (a) Viscous contribution [the first term in Eq. (53)] by setting $\phi = \pi/2$ and $d_A = d_B$. The case for a viscous fluid is plotted by the black line. (b) Elastic contribution [the second term in Eq. (53)] by setting $\phi = 0$ and $d_A \neq d_B$. The case for an elastic medium is plotted by the black line. Reprinted from Ref. [19]. © 2017 The Physical Society of Japan.

obtain its average as

$$\bar{V} = \frac{3a_1 a_2 (a_1 - a_2) d^2 \Omega}{4\ell^2 (a_1 + a_2)^2 \eta_0} \eta''[\Omega]. \quad (56)$$

This result shows that a reciprocal two-sphere microswimmer can swim in a viscoelastic fluid when the sphere sizes are different, i.e., $a_1 \neq a_2$. Similar to the first case in Eq. (55), \bar{V} depends only on $\eta''[\Omega]$ representing the elastic contribution. These two examples further confirm that the scallop theorem can be generalized for viscoelastic fluids because various reciprocal deformations of a microswimmer can still induce its locomotion.

IX. THREE-SPHERE MICROWIMMER IN A STRUCTURED FLUID

The locomotion of a microswimmer discussed in the previous section is valid for homogeneous viscoelastic fluids without any internal structures. However, one of the characteristic features of soft matter is that it contains various intermediate mesoscopic structures and behaves as structured fluids [63]. The existence of such internal length scales significantly affects the rheological properties of structured fluids [64]. In this section, we address the effects of intermediate structures of the surrounding viscoelastic fluid on the locomotion of a three-sphere microswimmer as shown in Fig. 1(h) [21]. Because a three-sphere microswimmer is characterized by its own size (the sphere size a and the average arm length ℓ), the swimming velocity depends on the relative magnitudes of the swimmer's size and the characteristic length of the surrounding fluid.

Consider a viscoelastic structured fluid with a characteristic length scale κ^{-1} and a time scale τ_v . We assume that the frequency-dependent one-point and two-point mobilities are expressed by the following scaling forms:

$$\mu[a, \omega] = \frac{\hat{\mu}[\kappa a, \omega \tau_v]}{6\pi\eta_0 a}, \quad M[r, \omega] = \frac{\hat{M}[\kappa r, \omega \tau_v]}{4\pi\eta_0 \ell}, \quad (57)$$

where $\hat{\mu}$ and \hat{M} are the dimensionless scaling functions and η_0 is the zero-frequency shear viscosity as before. Unlike the homogeneous viscoelastic fluid, the mobilities μ and M for a structured fluid are assumed to be written by the scaling functions that depend on the combinations κa and κr . Using these scaling functions, we write down the equation of motion for a three-sphere microswimmer in a structured fluid. Then, the swimming velocity can generally be obtained in terms of $\hat{\mu}$ and \hat{M} , and we obtain both the viscous and elastic contributions as in the previous section [21].

To illustrate the importance of intermediate length scales in structured fluids, we consider a polymer gel described by the two-fluid model [65, 66]. There are two dynamical fields in this model: the displacement field \mathbf{u} of the elastic network and the velocity field \mathbf{v} of the permeating fluid [see Fig. 1(h)]. When inertial effects are neglected, the linearized coupled equations for a polymer gel are given by

$$G\nabla^2 \mathbf{u} + \left(K + \frac{G}{3}\right) \nabla(\nabla \cdot \mathbf{u}) - \Lambda \left(\frac{\partial \mathbf{u}}{\partial t} - \mathbf{v}\right) = 0, \quad (58)$$

$$\eta \nabla^2 \mathbf{v} - \nabla P - \Lambda \left(\mathbf{v} - \frac{\partial \mathbf{u}}{\partial t}\right) + \mathbf{f} = 0, \quad (59)$$

where G and K are the shear and compression moduli of the elastic network, respectively, η is the shear viscosity of the fluid, P is the pressure, and \mathbf{f} is the external force density acting on the fluid component. The elastic and fluid components are coupled via the mutual friction terms characterized by the friction coefficient Λ . When the volume fraction of the elastic component is small, we further require the incompressibility condition, $\nabla \cdot \mathbf{v} = 0$. The above two-fluid model contains

the characteristic length $\kappa^{-1} = (\eta/\Lambda)^{1/2}$ and the characteristic time $\tau_v = \eta/G$. The former length scale roughly corresponds to the mesh size of a polymer network, and the latter time scale sets the viscoelastic relaxation time.

Diamant calculated the self-mobility of a sphere in a two-fluid gel under ‘‘a sticking fluid and a free network’’ boundary condition at the surface of the sphere [67]. On the other hand, the current authors previously obtained a general expression for the coupling mobility connecting the velocity \mathbf{v} and the force \mathbf{f} in the two-fluid model [68, 69]. Using these results, we calculated the swimming velocity of a three-sphere microswimmer in a two-fluid gel as the sum of the viscous and elastic contributions [21]. Because the surrounding gel is characterized by the network mesh size, κ^{-1} , the following three different situations can be distinguished under the condition $a \ll \ell$: (i) a large swimmer when $\kappa a \gg 1$ and $\kappa \ell \gg 1$, (ii) a medium swimmer when $\kappa a \ll 1$ and $\kappa \ell \gg 1$, and (iii) a small swimmer when $\kappa a \ll 1$ and $\kappa \ell \ll 1$.

In the following, we briefly discuss the case of a large swimmer [21]. The behavior of the viscous contribution for a large swimmer exhibits a non-monotonic dependence on the frequency Ω [see Eq. (7)]. A careful analysis reveals that it behaves as $\Omega \rightarrow \Omega^{-1/2} \rightarrow \Omega \rightarrow \Omega^{-1} \rightarrow \Omega$ as Ω increases. This non-monotonic behavior is more pronounced for larger sphere sizes. On the other hand, the frequency dependence of the elastic contribution crosses over as $\Omega^2 \rightarrow \Omega^0$. Several asymptotic expressions were also obtained. For example, in the limit of $\Omega \tau_v \rightarrow 0$, the viscous contribution becomes

$$\bar{V} = \frac{31a^3 d_A d_B \Omega}{144\ell^4} \sin \phi, \quad (60)$$

showing different dependence on a and ℓ compared to Eq. (8) for a three-sphere microswimmer in a purely viscous fluid.

X. OTHER GENERALIZATIONS AND OUTLOOK

In this article, we have reviewed various extensions of the three-sphere microswimmer. There are other extensions such as the case when one of the spheres has a larger radius [24, 25] or when the three spheres are arranged in a triangular configuration [70]. Montino and DeSimone considered the case, in which one arm is periodically actuated while the other is replaced by a passive elastic spring [71]. It was shown that such a microswimmer exhibits a delayed mechanical response of the passive spring with respect to the active arm. Later, they analyzed the motion of a three-sphere swimmer with arms having active viscoelastic properties mimicking muscular contraction [72]. Later, Nasouri *et al.* discussed the motion of an elastic two-sphere microswimmer, in which one of the spheres is a neo-Hookean solid [73].

Golestanian and Ajdari proposed a different type of stochastic microswimmer for which the configuration space of a swimmer generally consists of a finite number of distinct states [74, 75]. A similar idea was employed by Sakaue *et al.* who discussed the propulsion of molecular machines or active proteins in the presence of hydrodynamic interactions [76].

Later, Huang *et al.* considered a modified three-sphere swimmer in a two-dimensional viscous fluid [77]. In their model, the spheres are connected by two springs, the lengths of which are assumed to depend on the discrete states that are cyclically switched.

A model of a three-disk microswimmer in a quasi-two-dimensional supported membrane has been discussed [78]. Due to the presence of the hydrodynamic screening length in the quasi-two-dimensional fluid [79, 80], the geometric factor appearing in the average velocity exhibits three different asymptotic behaviors depending on the microswimmer size and the screening length. This is in sharp contrast with a microswimmer in a three-dimensional bulk fluid that exhibits only a single scaling behavior. The swimming behaviors of a three-sphere microswimmer near a wall were also discussed [81].

The future extensions of the three-sphere microswimmer will involve combining it with other advanced technologies,

such as nanotechnology, materials science, and artificial intelligence, to create a more sophisticated and versatile micro-robot [82–85]. These extensions could enable the microswimmer to perform even more complex tasks, such as targeted drug delivery to specific cells or tissues, or navigating through the human body to locate and repair damaged tissues.

ACKNOWLEDGMENTS

We thank K. Era, K. Ishimoto, H. Kitahata, A. Kobayashi, Y. Koyano, L.-S. Lin, R. Okamoto, and I. Sou for useful discussions and previous collaborations. K.Y. acknowledges the support by Grant-in-Aid for JSPS Fellows (No. 22KJ1640) from the Japan Society for the Promotion of Science. S.K. acknowledges the support by National Natural Science Foundation of China (Nos. 12274098 and 12250710127) and the startup grant of Wenzhou Institute, University of Chinese Academy of Sciences (No. WIUCASQD2021041).

-
- [1] E. Lauga and T. R. Powers, *Rep. Prog. Phys.* 72, 096601 (2009).
 [2] E. M. Purcell, *Am. J. Phys.* 45, 3 (1977).
 [3] K. Ishimoto and M. Yamada, *SIAM J. Appl. Math.* 72, 1686 (2012).
 [4] A. Najafi and R. Golestanian, *Phys. Rev. E* 69, 062901 (2004).
 [5] R. Golestanian and A. Ajdari, *Phys. Rev. E* 77, 036308 (2008).
 [6] M. Leoni, J. Kotar, B. Bassetti, P. Cicuta, and M. C. Lagomarsino, *Soft Matter* 5, 472 (2009).
 [7] G. Grosjean, M. Hubert, G. Lagubeau, and N. Vandewalle, *Phys. Rev. E* 94, 021101(R) (2016).
 [8] G. Grosjean, M. Hubert, and N. Vandewalle, *Adv. Colloid Interface Sci.* 255, 84 (2018).
 [9] J. Pande and A.-S. Smith, *Soft Matter* 11, 2364 (2015).
 [10] J. Pande, L. Merchant, T. Krüger, J. Harting, and A.-S. Smith, *New J. Phys.* 19, 053024 (2017).
 [11] K. Yasuda, Y. Hosaka, M. Kuroda, R. Okamoto, and S. Komura, *J. Phys. Soc. Jpn.* 86, 093801 (2017).
 [12] S. Ziegler, M. Hubert, N. Vandewalle, J. Harting, and A.-S. Smith, *New J. Phys.* 21, 113017 (2019).
 [13] Y. Hosaka, K. Yasuda, I. Sou, R. Okamoto, and S. Komura, *J. Phys. Soc. Jpn.* 86, 113801 (2017).
 [14] K. Yasuda, Y. Hosaka, I. Sou, and S. Komura, *J. Phys. Soc. Jpn.* 90, 075001 (2021).
 [15] A. Kobayashi, K. Yasuda, L.-S. Lin, I. Sou, Y. Hosaka, and S. Komura, *J. Phys. Soc. Jpn.* 92, 034803 (2023).
 [16] T. G. Mason and D. A. Weitz, *Phys. Rev. Lett.* 74, 1250 (1995).
 [17] F. Gittes, B. Schnurr, P. D. Olmsted, F. C. MacKintosh, and C. F. Schmidt, *Phys. Rev. Lett.* 79, 3286 (1997).
 [18] E. M. Furst and T. M. Squires, *Microrheology* (Oxford University Press, Oxford, 2017).
 [19] K. Yasuda, R. Okamoto, and S. Komura, *J. Phys. Soc. Jpn.* 86, 043801 (2017).
 [20] K. Yasuda, M. Kuroda, and S. Komura, *Phys. Fluids* 32, 093102 (2020).
 [21] K. Yasuda, R. Okamoto, and S. Komura, *EPL* 123, 34002 (2018).
 [22] K. Era, Y. Koyano, Y. Hosaka, K. Yasuda, H. Kitahata, and S. Komura, *EPL* 133, 34001 (2021).
 [23] M. Kuroda, K. Yasuda, and S. Komura, *J. Phys. Soc. Jpn.* 88, 054804 (2019).
 [24] R. Golestanian, *Eur. Phys. J. E* 25, 1 (2008).
 [25] B. Nasouri, A. Vilfan, and R. Golestanian, *Phys. Rev. Fluids* 4, 073101 (2019).
 [26] J. Happel and H. Brenner, *Low Reynolds Number Hydrodynamics* (Prentice-Hall, Englewood Cliffs, NJ, 1965).
 [27] A. Shapere and F. Wilczek, *J. Fluid Mech.* 198, 557 (1989).
 [28] K. Yasuda and S. Komura, *Phys. Rev. E* 103, 062113 (2021).
 [29] Y. Hosaka and S. Komura, *Biophys. Rev. Lett.* 17, 51 (2022).
 [30] M. Doi, *Soft Matter Physics* (Oxford University, Oxford, 2013).
 [31] A. Y. Grosberg and J.-F. Joanny, *Phys. Rev. E* 92, 032118 (2015).
 [32] K. Sekimoto, *Stochastic Energetics* (Springer, Berlin Heidelberg, 2010).
 [33] M. Yang, A. Wysocki, and M. Ripoll, *Soft Matter* 10, 6208 (2014).
 [34] H.-R. Jiang, N. Yoshinaga, and M. Sano, *Phys. Rev. Lett.* 105, 268302 (2010).
 [35] C. Scheibner, A. Souslov, D. Banerjee, P. Surówka, W. T. M. Irvine, and V. Vitelli, *Nat. Phys.* 16, 475 (2020).
 [36] M. Fruchart, C. Scheibner, and V. Vitelli, *Annu. Rev. Condens. Matter Phys.* 14, 471 (2023).
 [37] K. Yasuda, A. Kobayashi, L.-S. Lin, Y. Hosaka, I. Sou, and S. Komura, *J. Phys. Soc. Jpn.* 91, 015001 (2022).
 [38] K. Yasuda, K. Ishimoto, A. Kobayashi, L.-S. Lin, I. Sou, Y. Hosaka, and S. Komura, *J. Chem. Phys.* 157, 095101 (2022).
 [39] K. Ishimoto, C. Moreau, and K. Yasuda, *Phys. Rev. E* 105, 064603 (2022).
 [40] A. Kobayashi, K. Yasuda, K. Ishimoto, L.-S. Lin, I. Sou, Y. Hosaka, and S. Komura, *J. Phys. Soc. Jpn.* 92, 074801 (2023).
 [41] J. B. Weiss, *Tellus A* 55, 208 (2003).
 [42] J. B. Weiss, *Phys. Rev. E* 76, 061128 (2007).
 [43] I. Sou, Y. Hosaka, K. Yasuda, and S. Komura, *Phys. Rev. E* 100, 022607 (2019).
 [44] I. Sou, Y. Hosaka, K. Yasuda, and S. Komura, *Physica A* 562, 125277 (2021).
 [45] C. Battle, C. P. Broedersz, N. Fakhri, V. F. Geyer, J. Howard, C. F. Schmidt, and F. C. MacKintosh, *Science* 352, 604 (2016).
 [46] F. S. Gnesotto, F. Mura, J. Gladrow, and C. P. Broedersz, *Rep.*

- Prog. Phys. 81, 066601 (2018).
- [47] Y. Kuramoto, *Chemical Oscillations, Waves, and Turbulence* (Springer-Verlag, New York, 1984).
- [48] J. A. Acebrón, L. L. Bonilla, C. J. Pérez Vicente, F. Ritort, and R. Spigler, *Rev. Mod. Phys.* 77, 137 (2005).
- [49] A. Najafi and R. Golestanian, *EPL* 90, 68003 (2010).
- [50] C. M. Pooley, G. P. Alexander, and J. M. Yeomans, *Phys. Rev. Lett.* 99, 228103 (2007).
- [51] M. Farzin, K. Ronasi, and A. Najafi, *Phys. Rev. E* 85, 061914 (2012).
- [52] S. Ziegler, T. Scheel, M. Hubert, J. Harting, and A.-S. Smith, *New J. Phys.* 23, 073041 (2021).
- [53] E. Lauga, *EPL* 86, 64001 (2009).
- [54] M. P. Curtis and E. A. Gaffney, *Phys. Rev. E* 87, 043006 (2013).
- [55] J. Teran, L. Fauci, and M. Shelley, *Phys. Rev. Lett.* 104, 038101 (2010).
- [56] T. Qiu, T.-C. Lee, A. G. Mark, K. I. Morozov, R. Munster, O. Mierka, S. Turek, A. M. Leshansky, and P. Fischer, *Nat. Commun.* 5, 5119 (2014).
- [57] K. Ishimoto and E. A. Gaffney, *J. Fluid Mech.* 831, 228 (2017).
- [58] G. Li, E. Lauga, and A. M. Ardekani, *J. Non-Newtonian Fluid Mech.* 297, 104655 (2021).
- [59] S. E. Spagnolie and P. T. Underhill, *Annu. Rev. Condens. Matter Phys.* 14, 381 (2023).
- [60] K. Qin and O. S. Pak, *Phys. Rev. Fluids* 8, 033301 (2023).
- [61] R. Granek, *Soft Matter* 7, 5281 (2011).
- [62] J. C. Crocker, M. T. Valentine, E. R. Weeks, T. Gisler, P. D. Kaplan, A. G. Yodh, and D. A. Weitz, *Phys. Rev. Lett.* 85, 888 (2000).
- [63] T. A. Witten and P. Pincus, *Structured Fluids* (Oxford University Press, Oxford, 2004).
- [64] R. G. Larson, *The Structure and Rheology of Complex Fluids* (Oxford University Press, Oxford, 1999).
- [65] P. G. de Gennes, *Macromolecules* 9, 587 (1976).
- [66] P. G. de Gennes, *Macromolecules* 9, 594 (1976).
- [67] H. Diamant, *Eur. Phys. J. E* 38, 32 (2015).
- [68] K. Yasuda, R. Okamoto, S. Komura, and A. S. Mikhailov, *EPL* 117, 38001 (2017).
- [69] K. Yasuda, R. Okamoto, and S. Komura, *Phys. Rev. E* 95, 032417 (2017).
- [70] R. Ledesma-Aguilar, H. Löwen, and J. M. Yeomans, *Eur. Phys. J. E* 35, 70 (2012).
- [71] A. Montino and A. DeSimone, *Eur. Phys. J. E* 42, 38 (2015).
- [72] A. Montino and A. DeSimone, *Acta Appl. Math.* 149, 53 (2017).
- [73] B. Nasouri, A. Khot, and G. J. Elfring, *Phys. Rev. Fluids* 2, 043101 (2017).
- [74] R. Golestanian and A. Ajdari, *Phys. Rev. Lett.* 100, 038101 (2008).
- [75] R. Golestanian, *Phys. Rev. Lett.* 105, 018103 (2010).
- [76] T. Sakaue, R. Kapral, and A. S. Mikhailov, *Eur. Phys. J. B* 75, 381 (2010).
- [77] M.-J. Huang, H.-Y. Chen, and A. S. Mikhailov, *Eur. Phys. J. E* 119, 35 (2012).
- [78] Y. Ota, Y. Hosaka, K. Yasuda, and S. Komura, *Phys. Rev. E* 97, 052612 (2018).
- [79] P. G. Saffman and M. Delbrück, *Proc. Natl. Acad. Sci. USA* 72, 3111 (1975).
- [80] E. Evans and E. Sackmann, *J. Fluid Mech.* 194, 553 (1988).
- [81] A. Daddi-Moussa-Ider, M. Lisicki, C. Hoell, and H. Löwen, *J. Chem. Phys.* 148, 134904 (2018).
- [82] A. C. H. Tsang, P. W. Tong, S. Nallan, and O. S. Pak, *Phys. Rev. Fluids* 5, 074101 (2020).
- [83] B. Hartl, M. Hübl, G. Kahl, and A. Zöttl, *Proc. Natl. Acad. Sci. USA* 118, e2019683118 (2021).
- [84] Z. Zou, Y. Liu, Y.-N. Young, O. S. Pak, and A. C. H. Tsang, *Commun. Phys.* 5, 158 (2022).
- [85] Y. Liu, Z. Zou, O. S. Pak, and A. C. H. Tsang, *Sci. Rep.* 13, 9397 (2023).